Construction and Building Materials 494 (2025) 143315

Contents lists available at ScienceDirect

Construction and Building Materials

journal homepage: www.elsevier.com/locate/conbuildmat

Comparative analysis of the fatigue characterisation of natural rock asphalt/SBS composite modified asphalt binders using time sweep test and linear amplitude sweep test

Liang Xiong [a], Kai Liu [a], Huda A. Kadhim [a,b], Dongyu Niu [a,*], Yangming Gao [c], Xueyan Liu [d]

[a] School of Materials Science and Engineering, Chang'an University, Xi'an 710061, China
[b] Roads and Transport Department, College of Engineering, University of Al-Qadisiyah, Al-Diwaniyah 00964, Iraq
[c] School of Civil Engineering and Built Environment, Liverpool John Moores University, Byrom Street, Liverpool L3 3AF, United Kingdom
[d] Section of Pavement Engineering, Department of Engineering Structures, Faculty of Civil Engineering and Geosciences, Delft University of Technology, Stevinweg 1, Delft 2628 CN, the Netherlands

ARTICLE INFO

Keywords:
Natural rock asphalt
Composite modified asphalt binders
Fatigue performance
The DSR-C model

ABSTRACT

Fatigue cracking is one of the most notable distresses in steel bridge deck pavement (SBDP), necessitating the development of high performance pavement materials to extend service life. In this paper, the fatigue resistance characteristics of natural rock asphalt (NRA)/SBS systematically evaluated. Twelve types of composite-modified asphalt binders were prepared by incorporating Iranian rock asphalt (IRA), Buton rock asphalt (BRA), and SBS as modifiers. IRA and BRA were added at 5 wt%, 10 wt%, and 15 wt%, while SBS was introduced at 2 wt% and 3 wt %. The modified asphalt binders subjected to time sweep (TS) test and linear amplitude sweep (LAS) test to comparatively analyze fatigue damage and fatigue life. DSR-C model was applied to calculate the fatigue crack length. The research also comparative evaluate differences and correlations between fatigue crack length indexes and conventional fatigue life indexes. The results showed that NRA enhanced the fatigue performance of modified asphalt binders. With the increase of NRA content, the fatigue properties of modified asphalt also become better. S_3I_{15} is better than other composite modified asphalt binders in both fatigue life and fatigue cracking indexes, demonstrating that it offers the best resistance to fatigue damage. The fatigue cracking index calculated by the DSR-based cracking (DSR-C) model could effectively evaluate the fatigue performance of NRA/SBS composite modified asphalt binders. NRA/SBS composite modified asphalt could be widely used in steel bridge deck pavement.

1. Introduction

In recent years, the consumption of bridge deck paving materials has been increasing, and with it, the problem of fatigue cracking due to insufficient fatigue resistance of steel bridge deck paving (SBDP) materials has also increased [1]. In order to meet the green and low-carbon requirements of high-quality development, it is imperative to reduce the incidence of bridge deck deterioration and operation and maintenance costs, and to improve the performance and service life of bridge deck paving materials.

Currently, there are three main types of SBDP materials commonly used: Stone Mastic Asphalt (SMA) [2], Epoxy Asphalt (EA) [3], and Guss Asphalt (GA) [4]. SMA has good high and low temperature performance, and it is widely used in highway paving projects with mature technology, relatively low cost and short construction period [5]. EA is mainly categorized into two main types: Warm Epoxy Asphalt (WEA) in the U.S. and China, and Hot Epoxy Asphalt (HEA) in Japan. EA is mostly applied to steel bridge decks with complex stress conditions and can be composited with SMA and other materials [6]. However, double-layer EA is characterised by high cost, complicated construction, and difficult to treat after the occurrence of disease, and the existence of these objective reasons limits the application of EA.

Compared with SMA and EAM, GA has the advantages of good adhesion and excellent fatigue resistance, and thus has been focused on by researchers. GA is a special steel bridge deck paving material, which relies on its own mobility to pave and mold, without the need for milling. GA also has good waterproofing properties and strong synergistic deformation ability with steel plates [7]. However, to ensure that GA has

* Corresponding author.
E-mail addresses: niudongyu_1984@chd.edu.cn, niudongyu_1984@163.com (D. Niu).

https://doi.org/10.1016/j.conbuildmat.2025.143315
Received 18 April 2025; Received in revised form 13 July 2025; Accepted 21 August 2025
Available online 27 August 2025

sufficient adhesion, it is often mixed with a high percentage of SBS, which can lead to higher costs. Economical considerations have brought natural rock asphalt(NRA), a material that ensures fluidity at a lower cost, into the view of researchers [8].

The main types of NRA are Trinidad lake Asphalt (TLA), Qingchuan rock asphalt (QRA), Buton rock asphalt (BRA), and Iranian rock asphalt (IRA). The properties of these bitumens, such as softening point and needle penetration, vary according to origin and ore body characteristics. Scholars have found that TLA has significantly enhanced the anti-aging properties of asphalt binders, QRA can improve the high temperature performance of asphalt binders [9], BRA has a good adsorption properties of asphalt binders [10], IRA has a high viscosity and can effectively improve the asphalt binders resistance to high temperature deformation [11].

NRA can improve the adhesion and fatigue properties of matrix asphalt binders, which coincides with the needs of researchers [12]. But the current application of NRA in GA is more related to the physical properties of NRA modified asphalt binders, mixture road performance, and construction performance [13]. There is a lack of research on the fatigue performance of NRA modified asphalt binders, as well as on the influence of fatigue damage on rheological parameters and fatigue crack propagation characteristics. This limitation restricts the widespread use of NRA.

Therefore, the fatigue performance of modified bitumen can be evaluated by adopting appropriate fatigue test and corresponding indexes, which can effectively assess the applicability of NRA modified bitumen in the application of SBDP, and provide various references for the design of modified asphalt binders.

For the characterisation and indexing of asphalt fatigue performance, the Strategic Highway Research Program (SHRP) proposed a fatigue parameter ($|G^*|\cdot sin\delta$) in the Superior Performing Asphalt Pavement (Superpave) specification. This parameter is used to evaluate asphalt binders fatigue performance at medium temperatures, where G^* represents the complex shear modulus and δ represents the phase angle. Both values can be obtained from the dynamic shear rheometer (DSR) test, and the smaller the value of $|G^*|\cdot sin\delta$, the greater the asphalt binders resistance to fatigue cracking [14].

However, it is found that the SHRP fatigue parameters do not correlate well with the fatigue life of modified asphalt binders, mainly because they are measured within the asphalt binders viscoelastic range without considering damage effects. Consequently, in a follow-up study, the time sweep (TS) repetitive cyclic loading test was introduced in the National Cooperative Highway Research Programme (NCHRP) to study the fatigue performance of asphalt binders [15], and the TS test has been widely used to determine the fatigue damage criterion for asphalt binders [16]. Some studies have evaluated the fatigue performance of asphalt mortar by using empirical fatigue index N_{f50}, phenomenological index $N_{f,G^*\times C}$, and energetic index N_{p20} through stress-controlled tests and strain-controlled tests in TS test [17]. Where N_{f50} refers to the fatigue life at which G^* decreases to 50 % of its initial value; $N_{f,G^*\times C}$ refers to the fatigue life corresponding to the point at which $G^*\times C$ peaks (C refers to the number of cycles); and N_{p20} refers to the fatigue life corresponding to the point at which the dissipated energy ratio (DER) deviates from the initial no-damage linear phase by 20 %.

Since TS test are generally time-consuming, the American Association of State Highway and Transportation Officials (AASHTO) develops an accelerated fatigue procedure, the linear amplitude sweep (LAS) test (AASHTO-TP101). This test is conducted at a constant temperature and frequency by increasing the strain amplitude in order to measure the fatigue damage limit of the asphalt binders and to calculate the fatigue life of the asphalt binders by using the S-VECD model. In recent research, there have also been studies on the calculation and prediction of asphalt binders fatigue crack length based on the rheological parameters obtained from the TS test and the LAS test, and the establishment of the DSR-C model to evaluate the fatigue performance of modified asphalt binders from the mechanical point of view of crack expansion [18].

Table 1
SK70# road petroleum asphalt technical parameters.

Test		Values	Standard requirements	Testing method
Penetration at 25 ℃/ 0.1 mm		68	60–80	T 0604-2011
Softening point / ℃		53.5	≥46	T 0606-2011
Ductility at 15 °C/ cm		>100	≥100	T 0605-2011
Density at 15 °C / (g·cm^{-3})		1.039	Record of actual measurements	T 0603-2011
Viscosity at 135 ℃/ (Pa·s)		2.598	≤3	T 0619-2011
Thin film oven test (TFOT)	Quality loss / %	−0.501	−0.8–0.8	T 0610-2011
	Penetration ratio / %	71	≥61	T 0604-2011
	Residual ductility at 15 ℃/ cm	21	≥15	T 0605-2011

In summary, the current research is less involved in obtaining the fatigue damage parameters before and after the fatigue damage of NRA/SBS composite modified asphalt binders, and there is a lack of effective means of exploring the fatigue characterisation of NRA/SBS composite modified asphalt binders in the field of SBDP. At same time, for the NRA, the TLA is costly, whereas the QRA has high temperature sensitivity. The BRA and IRA are excellent at enhancing the performance of modified asphalt and are very suitable for preparing it for the GA used in SBDP [19,20].

Therefore, this paper starts from the fatigue properties of NRA/SBS composite modified asphalt binders, BRA and IRA were selected to prepare twelve types of NRA/SBS composite modified asphalt binders. LAS and TS tests were carried out on NRA/SBS composite modified asphalt binders. According to the results of TS test and LAS test, different fatigue indexes were selected to evaluate the fatigue performance of NRA/SBS modified asphalt binders. The DSR-C model suitable for NRA/SBS modified asphalt binders was established, and the NRA/SBS composite modified asphalt binders with better fatigue performance was screened out. In addition, this study analyzes the differences and correlations between conventional fatigue life indexes and fatigue cracking indexes. The results of this paper can provide theoretical support for the application of NRA in SBDP.

2. Materials and methods

2.1. Materials

In this study, SK70# road petroleum asphalt was selected as the base asphalt, and its basic technical, which were determined according to the Chinese standard JTG E20-2011 [21], are shown in Table 1. NRA/SBS composite modified asphalt binders used in NRA was selected from BRA (Fig. 1(a)) and IRA (Fig. 1(b)). The NRA used in this study were in solid granular form and were added to the matrix asphalt binders as modifiers. Its basic technical parameters are determined according to the Chinese standard JT/T 860.5-2014 [22], are shown in Table 2. T161B linear SBS (Fig. 1(c)), produced by Dushanzi Petrochemicals in Xinjiang, was used as the preparatory material, with an embedding ratio of 30:70. As for the modified asphalt polymer matrix, its basic technical parameters are shown in Table 3.

2.1.1. Sample preparation

The base asphalt was kept at a temperature of 175 °C and the SBS modifier was added. Then the high-speed shear was set to operate at 5000 rpm. The mixture was then sheared at a constant speed for one hour. Then, the NRA was added to the asphalt binders and the mixture was sheared for a further 30 min. Finally, the mixture was placed in an

Fig. 1. Raw materials.

Table 2
NRA basic technical parameters.

Types of rock asphalt	BRA		IRA	
Test indicators	Values	Standard requirements	Values	Standard requirements
Natural bitumen content/ %	25.4	≥18	85.3	-
Ash content/ %	14.7	≤15	0.8	≤1
Density (15°C) (g/ cm^3)	1.81	≥1.70, ≤1.90	1.03	-
Water content/ %	0.4	≤2	0.2	≤2

Table 3
T161B linear SBS technical parameters.

Technical item	Test result	Unit
Oil content	0	wt%
Styrene content	31	wt%
Volatile content	0.37	wt%
300 % tensile stress	2.47	MPa
Tensile strength	25.5	MPa
Elongation at break	750	%
Shore hardness	79	Shore A

Table 4
NRA/SBS modified asphalt binders sample abbreviation description.

NRA dopant	SBS dopant	
	2 wt% SBS	3 wt% SBS
5 wt% IRA	S_2I_5	S_3I_5
10 wt% IRA	S_2I_{10}	S_3I_{10}
15 wt% IRA	S_2I_{15}	S_3I_{15}
5 wt% BRA	S_2B_5	S_3B_5
10 wt% BRA	S_2B_{10}	S_3B_{10}
15 wt% BRA	S_2B_{15}	S_3B_{15}

oven at 165 °C for 30 min to complete the development process [23].

Table 4 shows the abbreviated names of the various NRA/SBS composite modified asphalt binders formulations. The composite modified asphalt binders samples used in this study were aged using PAV aging method for 20 h at 64 ℃ [24].

2.2. Test methods

2.2.1. Linear amplitude sweep test

The test temperature was set at 20 °C, the diameter of the asphalt binders is 8 mm, and the spacing of the parallel plates is 2 mm. Two repetitions of the test were conducted for each type of asphalt binders. The LAS test was carried out in two phases in the strain control mode. In the first stage, the specimens were subjected to frequency sweeping test with a strain amplitude of 0.1 % and a scanning frequency range of 0.2–30 Hz.

Based on the result of the frequency sweeping test, the damage analysis parameter α is determined to obtain the performance of the modified asphalt binders before damage, and this is used to evaluate the rheological properties of the modified asphalt binders. In the second stage, the oscillatory shear mode was selected, and the sinusoidal load amplitude was linearly increased from 0.1 % to 30 % over 300 s at a constant frequency (10 Hz) during 3100 loading cycles. The total test time was 310 s, the peak shear strain,peak shear stress, phase angle and complex shear modulus were recorded every 10 loading cycles (1 s) [25]. Modified asphalt binders was considered to fail when the initial modulus is reduced by 35 %, and the number of failure cycles was calculated using Eq. (1).

$$N_f = A \cdot (\gamma_p)^{-B} \tag{1}$$

Where N_f is the fatigue life; γ_p represents the amplitude of the applied shear strain.

A and B are VECD model coefficients which depending on the material properties. A represents the ability of the material to maintain its integrity during loading cycles and cumulative damage. This parameter is directly related to the energy storage modulus. If the energy storage modulus decreases during the loading cycle, then A decreases. It indicates that the asphalt binders has a lower ability to resist cumulative damage and maintain its integrity during the loading process [26]. According to Eq. (1), when the strain level is equal to 1, the fatigue life is equal to A. Therefore, A can be regarded as the fatigue life of asphalt binders at a strain level of 1 (100 %). Both A and B can be calculated by the mechanical model of damage evolution of viscoelastic materials in VECD theory (S-VECD model) as shown in Eqs. (2)–(5) [26].

$$D(t) = \sum_{i=1}^{N} [\pi {\gamma_0}^2 (C_{i-1} - C_i)]^{\frac{\alpha}{1+\alpha}} (t_i - t_{i-1})^{\frac{1}{1+\alpha}} \tag{2}$$

$$C(t) = C_0 - C_1 (D)^{C_2} \tag{3}$$

$$D_f = \left(\frac{C_0 - C@PeakStress}{C_1} \right)^{1/C_2} \tag{4}$$

$$A = \frac{f \cdot (D_f)^{1+\alpha(1-C_2)}}{[1+\alpha(1-C_2)] \cdot (\pi C_1 C_2)^{\alpha}}; B = 2\alpha \tag{5}$$

Where D represents damage density, γ_0 represents the applied strain during the test. t is the test time. α is the reciprocal of the slope of the storage modulus G'_0 with respect to the logarithm of angular frequency,

Table 5
LAS testing fatigue parameter results based on S-VECD model.

Asphalt binders	α	C_1	C_2	A ($\times 10^5$)	B
S_2I_5	1.288	0.052	0.629	2.332	−2.789
S_2I_{10}	1.291	0.059	0.664	3.997	−2.956
S_2I_{15}	1.342	0.071	0.641	6.432	−2.876
S_3I_5	1.478	0.023	0.712	2.875	−3.087
S_3I_{10}	1.432	0.095	0.779	4.156	−3.102
S_3I_{15}	1.498	0.019	0.746	7.231	−3.214
S_2B_5	1.298	0.038	0.689	1.987	−2.459
S_2B_{10}	1.295	0.041	0.658	4.054	−2.563
S_2B_{15}	1.335	0.065	0.691	6.873	−2.672
S_3B_5	1.488	0.027	0.728	2.677	−2.648
S_3B_{10}	1.510	0.083	0.752	4.438	−3.321
S_3B_{15}	1.512	0.057	0.703	7.148	−3.391

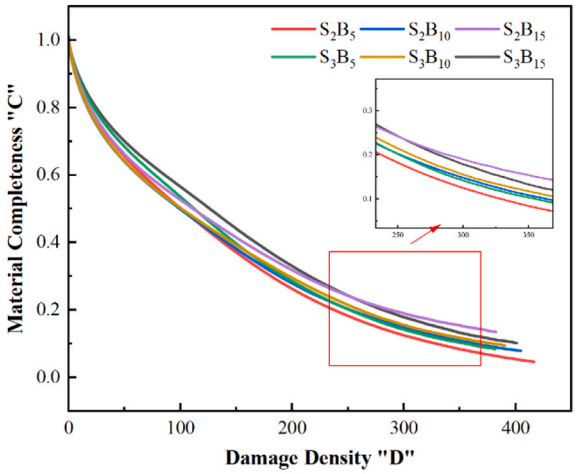

(a) BRA/SBS

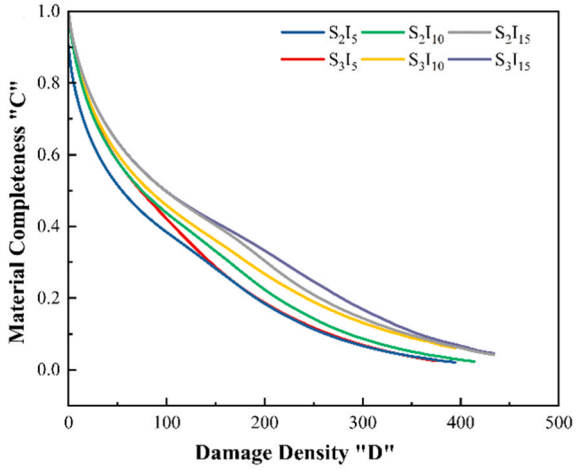

(b) IRA/SBS

Fig. 2. NRA/SBS composite modified asphalt binders D-C curve.

which calculated from frequency sweep data. $C(t)$ represents the ratio of the complex modulus of the sample at time t to the initial complex modulus, indicating material integrity. C_0 is the initial value of C, equal to 1. $C@PeakStress$ is the material integrity value corresponding to the peak stress. C_1 and C_2 are curve-fitting parameters. D_f represents the fatigue failure criterion. f is the test loading frequency.

2.2.2. Time sweep test

The TS test is a strain-controlled fatigue test that is performed at room temperature to ensure that fatigue failure of the asphalt binders material occurs by applying cyclic loading to the asphalt binders at low strain levels [27]. The DSR parallel loading plate used in this section of the test is 8 mm in diameter with a gap set at 2 mm. The samples were subjected to 54,000 cycles of loading at a temperature of 20 °C, a frequency of 10 Hz, and a strain control mode of 5 % in order to determine the complex shear modulus, phase angle, and other fatigue parameters of the samples under the failure-damage condition. The time-scan test is time-consuming, but it can be used to validate the results of the strain-frequency-scan test based on the S-VECD theory from the basic definition of fatigue life.

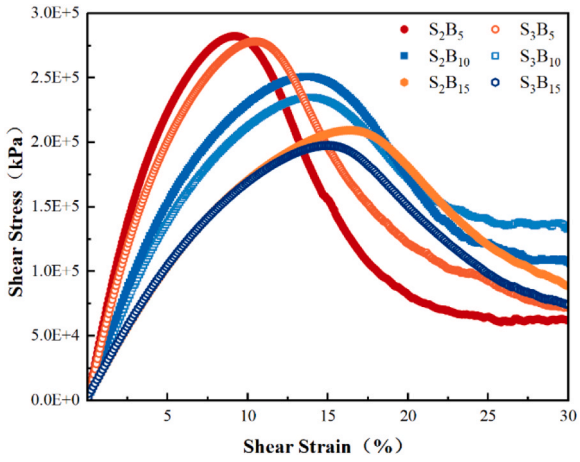

(a) BRA/SBS

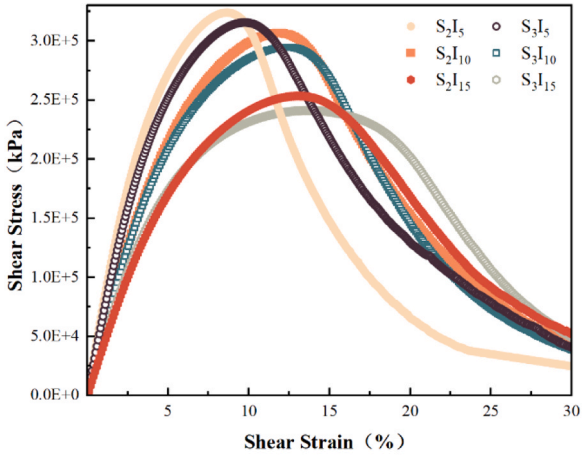

(b) IRA/SBS

Fig. 3. Strain-stress curve for NRA/SBS composite modified asphalt binders.

3. Results and discussion

3.1. Analysis of LAS test result

In this study, the fatigue parameters of each NRA/SBS composite modified asphalt binders were calculated by the S-VECD model.The results are given in Table 5.

The S-VECD model effectively measures the correlation between damage density D and material integrity C. The specific results are shown in Fig. 2. When the damage density D is kept constant, the increase in the value of C reflects better material integrity, implying that the asphalt binders material has better durability when subjected to

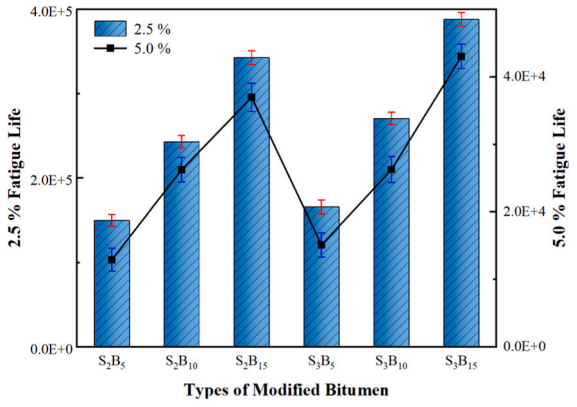

(a) BRA/SBS

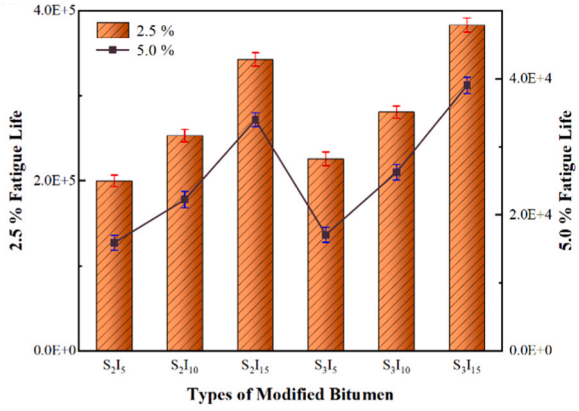

(b) IRA/SBS

Fig. 4. Fatigue life based on S-VECD model at different strain levels.

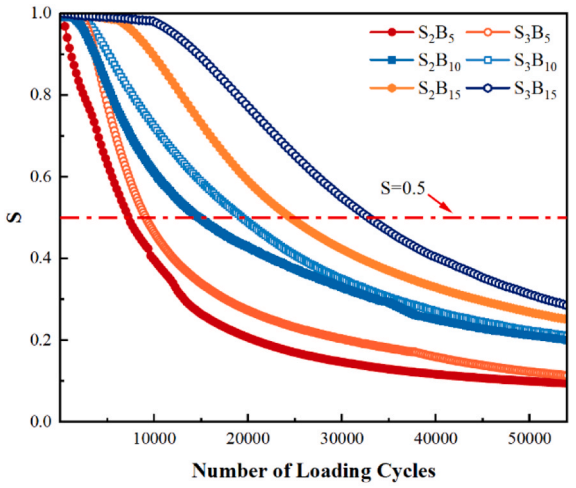

(a) BRA/SBS

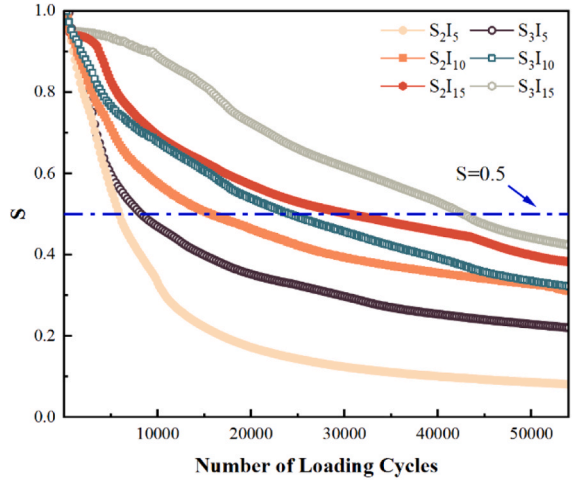

(b) IRA/SBS

Fig. 5. Normalised modulus ratio vs. loading cycles for composite modified asphalt binders.

more load cycles, and at the same time the fatigue resistance to damage is improved. As can be seen from the trend of the curve in the figure, where D is 0 the highest material integrity ($C = 1$), implying that the composite modified asphalt binders remains undamaged at this point in time. With the damage density D increases,the C value decreases. At $D = 400$, all composite modified asphalt binders C values decrease by more than 80 %, falling below 0.2.

At the same damage density, the C value increases with higher SBS and NRA content in the composite modified asphalt binders. When the C value is the same, the composite modified asphalt binders with higher content of SBS and NRA can withstand greater damage density. The material integrity of S_3B_{15}, S_2B_{15}, S_3I_{15}, and S_2I_{15} performs better when the NRA doping is up to 15 wt%, which indicates that the fatigue resistance of the asphalt binders has been enhanced by the composite effect of SBS and NRA. A possible reason for this situation is that the NRA is fully dissolved in the asphalt binders during the modification process. Its components of pure asphalt, mineral components and SBS together to participate in the modification process, so that the modified asphalt resistance to high temperature deformation ability to increase, and further enhance its fatigue resistance [20].

Fig. 3 shows the results of stress-strain curves for different composite modified asphalt binders samples. It can be seen that, with the increase of shear strain, the shear stress response of the composite modified asphalt binders samples reaches a peak at a certain point. This peak stress corresponds to the yield stress of the asphalt binders material. The shear strain at which this peak occurs is referred to as the yield strain. After the shear strain continues to increase and exceeds the yield strain, the shear stress decreases rapidly from the yield stress point, at this time, the asphalt binders material has undergone serious fatigue damage, the ability to withstand shear stress decreases dramatically.

For the peak stress value of each curve, it can be seen from the figure that the yield stress values of S_2B_5, S_3B_5, S_2I_5, and S_3I_5 are larger, which indicates that 5 wt% NRA modified asphalt binders lacks ductility and is more prone to brittle fracture. Different curves correspond to different peak values and their corresponding widths. The larger the peak yield stress value is, the narrower the peak width of the curve is. However SBS and NRA doping can obviously reduce the peak yield stress value, and the peak width is proportional to the dosage of SBS and NRA. Among them, which S_2B_{15}, S_3B_{15}, S_2I_{15}, S_3I_{15} have larger peak widths. This indicates that the composite modified asphalt binders has less strain dependence and better fatigue resistance due to the increase of SBS and NRA content.

The 2.5 % and 5.0 % shear strains used in this study represent the modified asphalt binders applied to low strength pavements and high strength, respectively. The predicted fatigue life of each NRA/SBS composite modified asphalt binders is calculated by the S-VECD theory for the two strain levels. The results are shown in Fig. 4. The fatigue life of the composite modified asphalt binders increases with the increase of the mass percentage of NRA under the same SBS doping level. At the same time, the fatigue life of composite modified asphalt binders increased when the SBS dosage is increased from 2 wt% to 3 wt%. S_3B_{15}

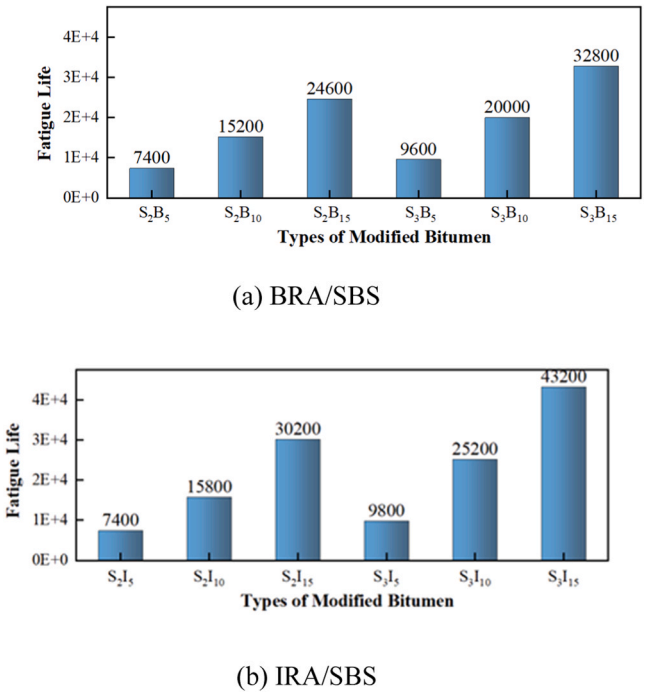

Fig. 6. Fatigue life based on complex modulus decay criterion.

and S_3I_{15} have the highest fatigue life at the same shear strain. Strain increased from 2.5 % to 5.0 %, the fatigue life of different types of composite modified asphalt binders has a large difference. And this difference is more obvious under the strain level of 5 %. The fatigue life of the same asphalt binders at 5.0 % is significantly lower than that at 2.5 %. It can be seen that high strain conditions on the fatigue life of composite modified asphalt binders are unfavourable, so in practical applications, there is a need to select composite modified asphalt binders according to the specific surface bearing conditions to ensure the durability of the road.

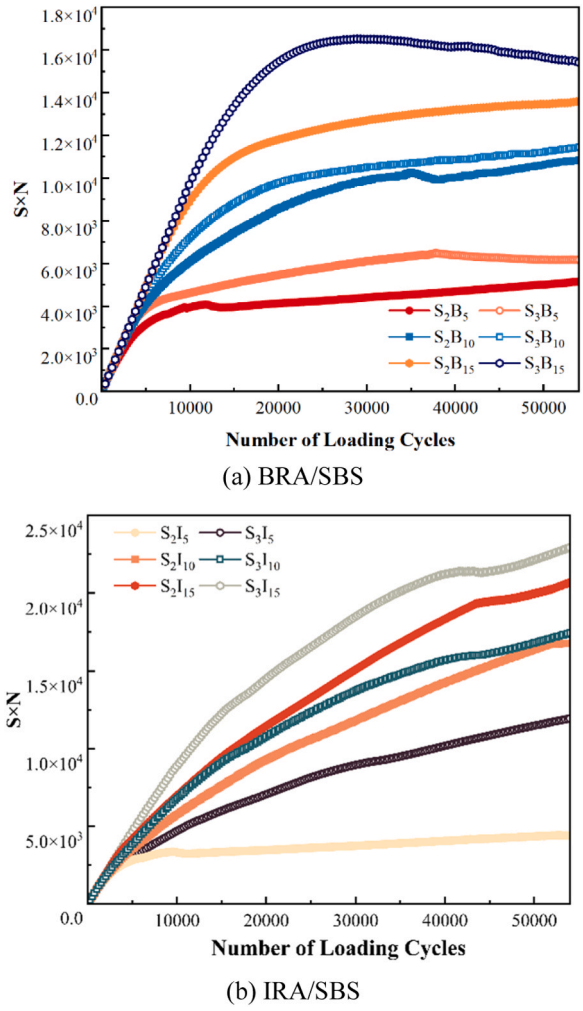

Fig. 7. Curve of $S\times N$ versus number of loading cycles.

3.2. Analysis of TS test result

3.2.1. The complex modulus decay criterion

The complex modulus decay criterion uses the number of loading cycles corresponding to the reduction of asphalt binders modulus to the initial 50 % as the fatigue life of the asphalt binders. For visual analysis, the normalised modulus ratio S is used as the research index. S is the ratio of the complex shear modulus under each loading cycle to the complex shear modulus measured under the first shear cycle, meaning the initial normalised modulus ratio of all asphalt binders types is $S = 1$. The curves shown in Fig. 5 presented the relationship between the S value and the number of loading cycles for each composite modified asphalt binders.

From the results in Fig. 5, it can be seen that the normalised modulus ratio curves of S_2B_{15} and S_3B_{15} are further to the right from the intersection point at $S = 0.5$ at 5 % strain level. The S value decays to 0.5 after 24,600 and 32,800 oscillatory loading cycles, respectively, which shows good fatigue resistance.

In addition, it can be seen from Fig. 5 that at the beginning of loading, the S curve for composite modified asphalt binders exhibits a short "platform area". As the dosage of SBS and NRA increases, the duration of the platform area extends. The plateau region of the S curve is more pronounced for S_2B_{15}, S_3B_{15}, S_2I_{15} and S_3I_{15}. This may be due to the compounding action of NRA and SBS, which improves the ability of the material to maintain its integrity.

When the number of loading cycles approaches 10,000, a sharp decline in the S curve begins to appear. In contrast, asphalts such as S_2B_5 and S_2I_5 demonstrate a downward trend at the start of the loading cycle. This suggests that the combined effect of NRA and SBS causes the fatigue damage node in the asphalt matrix to appear later. The fatigue lives which determined by complex modulus decay quasi-measurement of S_2I_{15} and S_3I_{15} are 30,200 and 43,200. This is superior to both S_2B_{15} and S_3B_{15}.

The predicted fatigue life results in Fig. 6 are consistent with the LAS test fatigue life results, showing an improvement in fatigue performance with increased SBS and NRA content. S curve platform area of S_2B_{15}, S_3B_{15}, S_2I_{15}, and S_3I_{15} is more obvious, while S_2B_5 and S_2I_5, and other asphalt binders types in the beginning of the loading cycle, show a decreasing trend. This indicates that the composite effect of NRA and SBS delays the appearance of the fatigue damage node of the asphalt binders matrix. This may be due to the increased asphaltene content in the modified asphalt binders. In the asphalt colloidal model, asphaltens are assumed to exist as associations of polar molecules, and the associations are not mobilized by addition of solvents such as n-heptanes. With the addition of natural rock asphalt, asphaltens and resins content increases. At the same time, saturates and aromatics content decreases. From the asphalt composition analysis, the addition of rock asphalt improves its temperature durability and high temperature performance. It further improves its fatigue resistance [28].

3.2.2. The $S\times N$ peak criterion

$S\times N$ is a phenomenological indicator. S is the normalised modulus ratio defined during the fatigue test and N is the number of loading cycles. The fatigue life calculated based on this fatigue criterion is

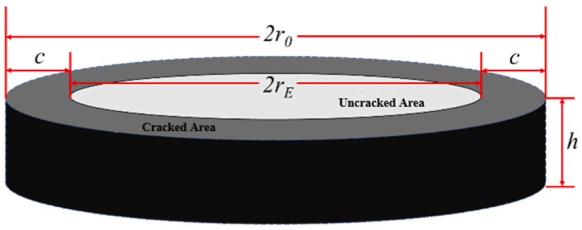

Fig. 8. Schematic diagram of cylindrical samples in DSR test.

defined as the number of loading cycles at which the asphalt binders reaches its highest $S\times N$ value.

From Fig. 7(a), the peaks of the $S\times N$ curves for all the composite-modified asphalt binders appeared in the plateau region. The S_3B_{15} peak was the largest, followed by the S_2B_{15} peak, while the S_2B_5 peak was the smallest and appeared at the earliest time. This suggests that increasing the dosage of SBS and BRA greatly increases the $S\times N$ peaks and delays their appearance. According to Fig. 7(b), the S_2I_5 peak appeared in a region similar to the plateau and the $S\times N$ value changed little with an increase in the number of loading cycles. Except for S_2I_5,

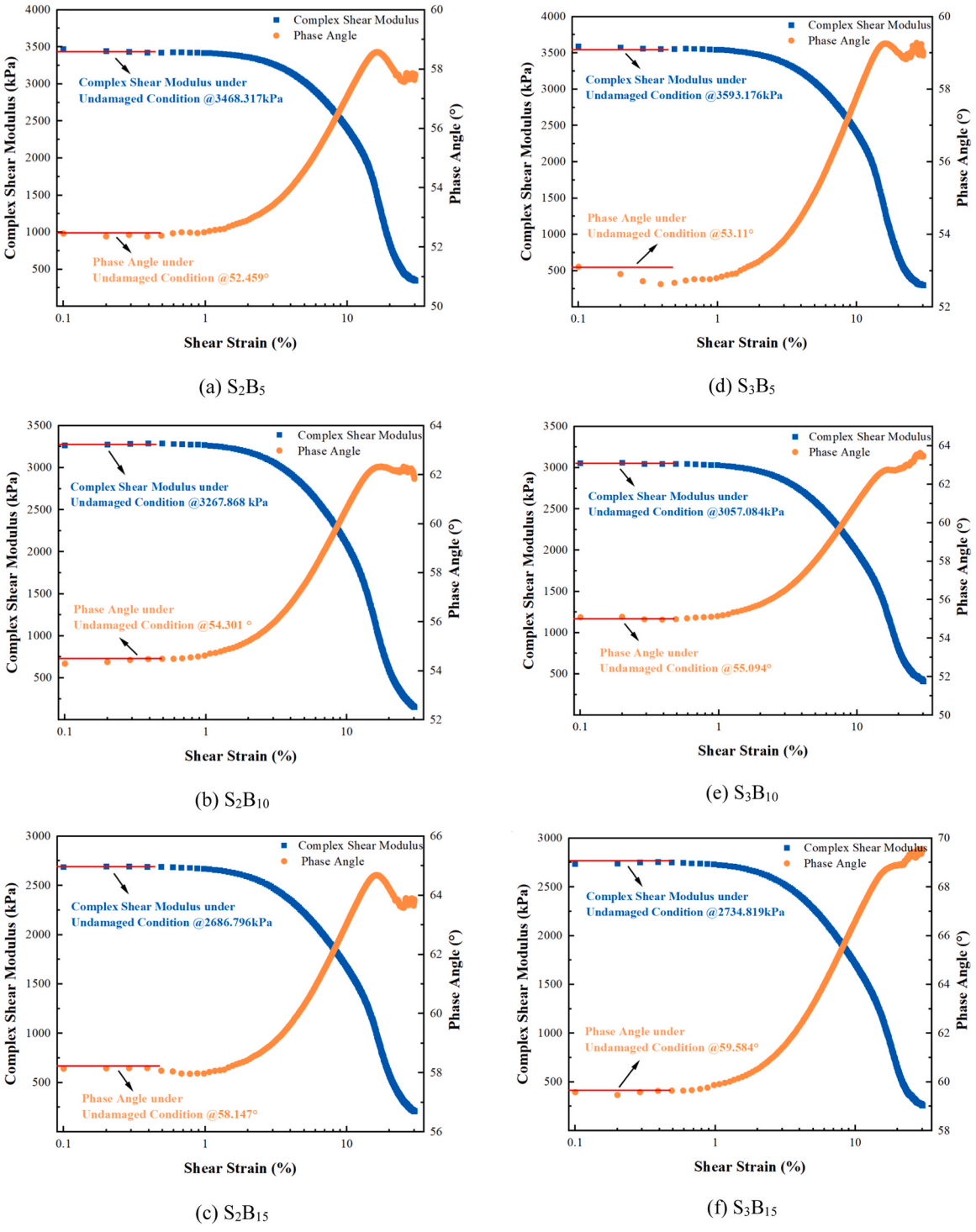

Fig. 9. $|G_0^*|$ and δ_0 for BRA/SBS.

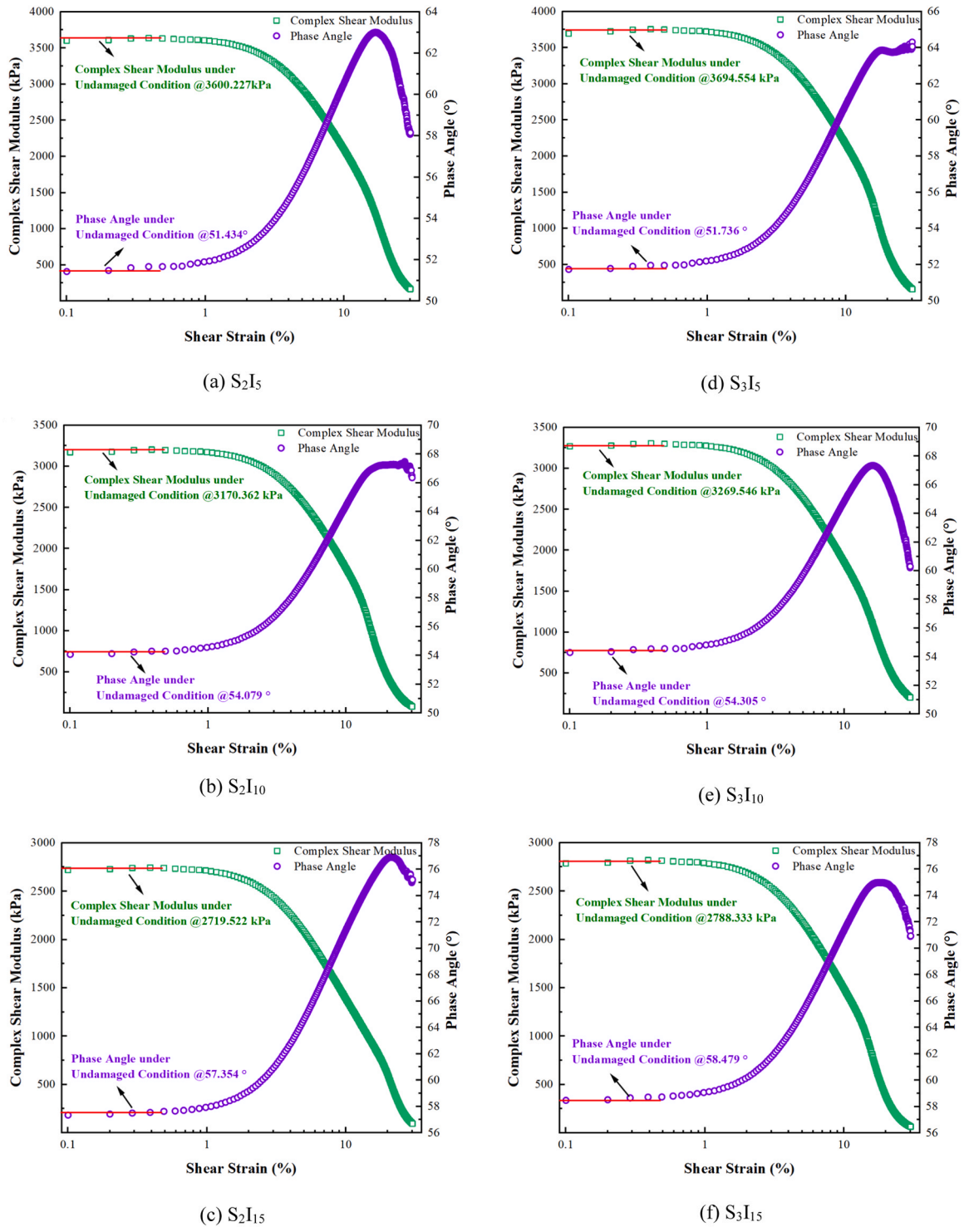

Fig. 10. $|G_0^*|$ and δ_0 for IRA/SBS.

the $S\times N$ curves of all the IRA/SBS composite modified asphalt binders showed a continuous upward trend and the peaks appeared with a clear lag.

It is worth noting that Some kinds of NRA/BRA asphalt binders did not reach the peak value of $S\times N$, which shows that the fatigue life of these asphalt binder would be much higher if the $S\times N$ criterion was considered. Therefore, the TS test should be carefully evaluated and finished after the peak of $S\times N$ is finally reached.

When the IRA doping is 10 %, the $S\times N$ values of S_2I_{10} and S_3I_{10} are significantly higher than those of S_2I_5 and S_3I_5. Furthermore, the $S\times N$ values of S_2I_{10} and S_3I_{10} show a tendency to be close to each other when the number of loading cycles is more than 45,000. The minor fluctuations observed in the $S\times N$ curves of S_2I_{15} and S_3I_{15} near the 45,000 cycles may be attributable to the decline in the phase angle of S_2I_{15} and S_3I_{15} prior to the termination of the shear cycles. In general, both the NRA and SBS composite asphalt binders demonstrate adequate fatigue resistance during the loading cycles. Furthermore, the fatigue resistance of the asphalt binder matrix is found to be positively influenced by the augmentation of SBS and NRA contents.

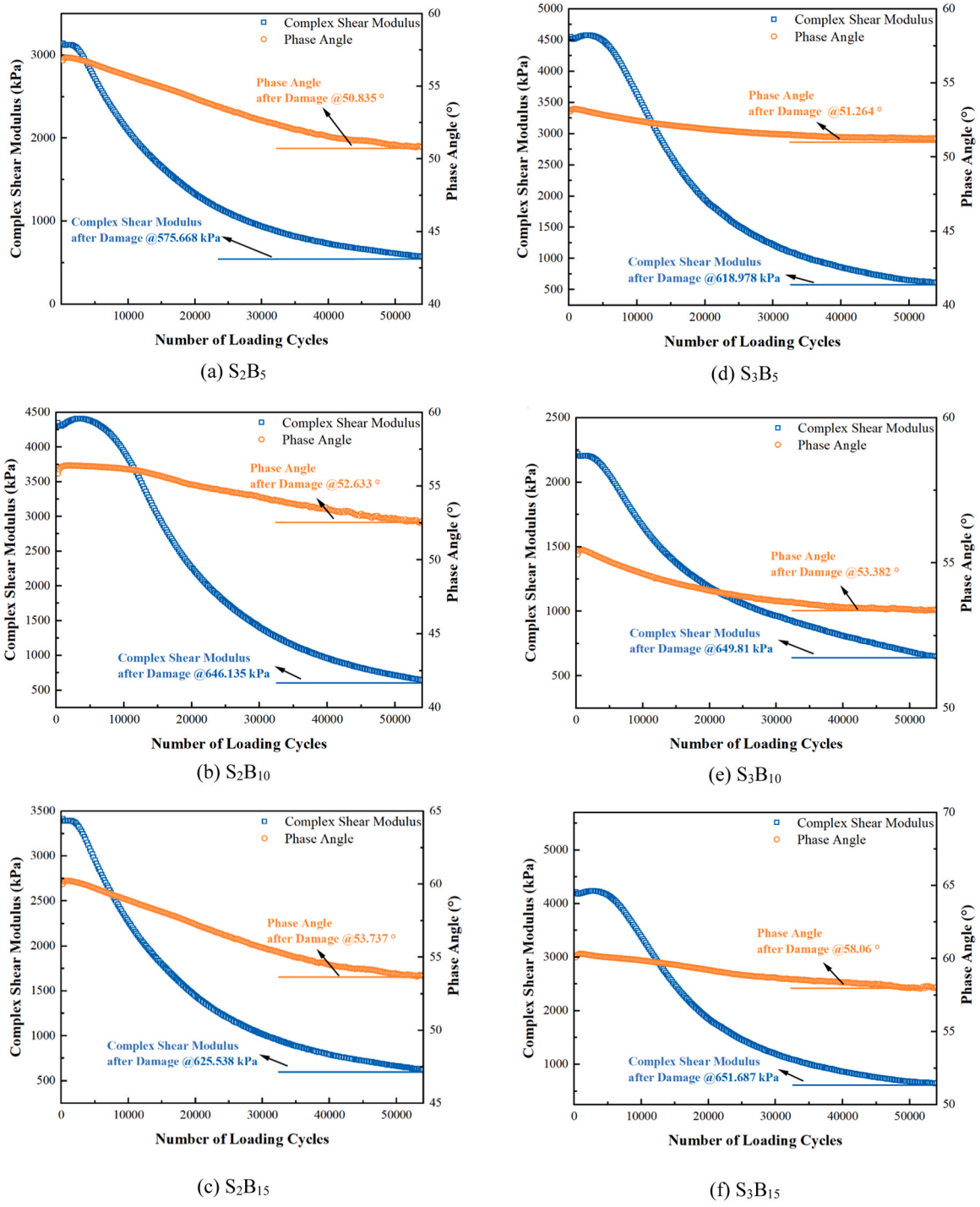

Fig. 11. $|G_N^*|$ and δ_N for BRA/SBS.

3.3. DSR-C fatigue damage model based on LAS and TS tests

Crack length can be used as a direct assessment of the fatigue cracking resistance of asphalt binders. In order to improve the accuracy of fatigue crack prediction in asphalt binders and to explain the cracking process of asphalt binders materials under rotational shear fatigue loading, a number of existing studies have begun to focus on the direct study of crack propagation in asphalt binders. For example, Hintz uses TS testing and digital visualisation in DSR to study trends in crack expansion in asphalt binders samples [25]. Shan used DSR testing and image analysis to determine internal crack expansion in asphalt binders samples during shear fatigue [17]. In these studies, Eq. (6) is used to predict the effective radius based on the fact that the measured torque (T) decreases with the number of loading cycles in the TS test. The crack length in the DSR test is determined by subtracting r_E determined by Eq. (6) from the original sample radius r_0.

$$r_E^4 = \frac{2TH}{\pi\theta\left|G_0^*\right|} \tag{6}$$

Where r_E is the effective radius shown in Fig. 8, representing the radius of the remaining uncracked area of the asphalt binders sample in the DSR test. T and θ are the torque and deflection angles measured by DSR. h is the height of the sample. And $|G_0^*|$ is the shear modulus of the

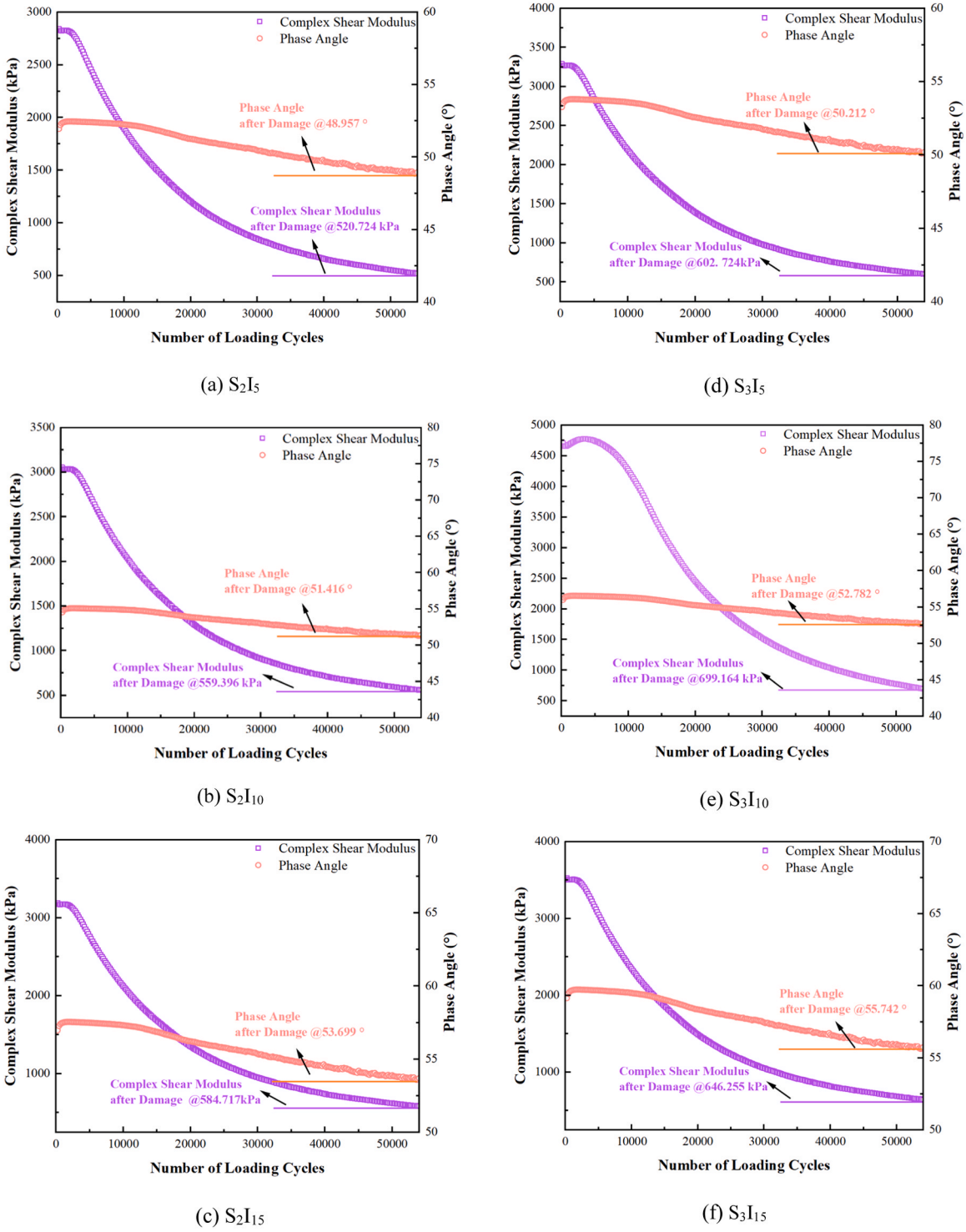

Fig. 12. $|G_N^*|$ and δ_N for IRA/SBS.

undamaged asphalt binders.

However, in the case of a relatively high number of load cycles, the calculated values of crack length are smaller than the measured values from the digital image analysis. This is mainly due to the fact that Eq. (6) is derived from the linear elastic stress-strain constitutive relationship in the undamaged state. Therefore it cannot be used to predict the effective radius resulting from fatigue crack growth in the damaged state. For the above reasons, Zhang and Gao et al. use the principle of damage mechanics and the rheological parameters of asphalt binders before and after fatigue damage obtained from LAS and TS tests to develop a DSR-based crack growth (DSR-C) model to predict the crack expansion of asphalt binders during the DSR test[27]. Thus, they provide a direct method to effectively quantify the fatigue resistance of asphalt binders. The DSR-C model adopts the principle of damage mechanics, principle of torque, and dissipated strain energy (DSE) equilibrium (Eqs. (7), (8)) and establishes a predictable crack expansion calculation formula (Eq. (9)) for asphalt binders under rotational shear fatigue loading.

$$\frac{\pi {r_0}^3}{2}\tau_{N\,\max} = \frac{\pi {r_E}^3}{2}\tau_{E\,\max} \tag{7}$$

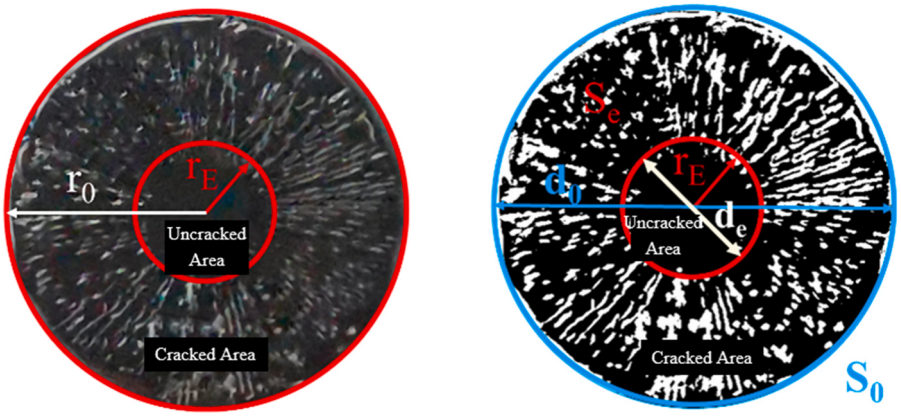

(a) (b)

Fig. 13. (a) Typical surface crack image of asphalt binder sample after TS test at 20 °C and 10 Hz; (b) Real crack morphology image of asphalt binder sample surface after treatment.

$$\int_0^{r_0} \pi\tau_N(r)^2 \frac{\sin\delta_N}{|G_N^*|}\cdot 2\pi r\cdot h\cdot dr = \int_0^{r_E} \pi\tau_E(r)^2 \frac{\sin\delta_0}{|G_0^*|}\cdot 2\pi r\cdot h\cdot dr \tag{8}$$

$$c = \left[1 - \left(\frac{|G_N^*|/\sin(\delta_N)}{|G_0^*|/\sin(\delta_0)}\right)^{\frac{1}{4}}\right] r_0 \tag{9}$$

Where $\tau_{N\,\max}$ is the maximum stress amplitude of the asphalt binder sample under damage conditions at the nth load cycle;$\tau_{E\,\max}$ is the maximum effective stress amplitude of the asphalt binder under undamaged conditions. $|G_0^*|$ and δ_0 are the dynamic modulus and phase angle of the asphalt binder under undamaged conditions. $|G_N^*|$ and δ_N are the dynamic modulus and phase angle of the asphalt binder under the nth loading cycle in time sweep.

3.3.1. Rheological parameters of asphalt binders before and after fatigue damage

The shear modulus $|G_0^*|$ as well as the phase angle δ_0 of the asphalt binders under undamaged conditions are obtained from the LAS test. The LAS fatigue damage test ranging from 0.1 % to 30 % test at temperature of 20 °C.

Figs. 9 and 10 show the variation curves of shear modulus $|G_0^*|$ and phase angle δ_0 with linear shear strain, measured during the LAS test for BRA/SBS and IRA/SBS composite modified asphalt binders, respectively. In all plots, the complex shear modulus shows a platform area and then decreases rapidly with increasing shear strain. The platform area corresponds to smaller shear strains which are around 1 %, and the complex shear modulus curve decreases the fastest after the shear strain exceeds 10 %.

For the phase angle curve, it is in the shear strain of 1 % near the platform area, and then increases rapidly. Upon reaching approximately 5 % strain levels in the shear process, both the complex shear modulus and the phase angle undergo observable alterations. When the shear strain reaches 10 %, the phase angle curve shows a sudden decreasing trend, with peak-like fluctuations observed in the figure. It can be seen that a shear strain of 10 % represents the cut-off point for the rapid decay of the rheological properties of the composite modified asphalt binders material.

Furthermore, comparative analysis revealed that the phase angle at which fatigue damage did not occur increased with increasing rock asphalt dosage. This finding is consistent with the change rule of the phase angle where fatigue damage occurs later, indicating that high rock bitumen dosage can improve the fatigue performance of modified asphalt. This hypothesis is supported by subsequent fatigue cracking experiments.

According to the $|G_0^*|$ as well as δ_0 results of NRA/SBS composite modified asphalt binders determined by the LAS test, the complex shear modulus and phase angle begin to show a significant trend of change at a strain level of 5 %. So the controlled strain level of the TS test is chosen to be 5 %, the test temperature is 20 °C, and the test frequency is 10 Hz. In fact, TS tests using 5 % and 7 % strain levels have been performed in the literature to study the fatigue damage behavior of asphalt [29,30]. In order to ensure that each composite modified asphalt binders under the loading conditions shows obvious fatigue damage, the loading cycle time of this test is set to 5400 s, so the total number of cycles is 54,000 times. Figs. 11 and 12 show the variation curves of post-breakage shear modulus $|G_N^*|$and phase angle δ_N with the number of loading cycles, measured during the TS test for BRA/SBS and IRA/SBS composite asphalt binders, respectively.

At the beginning of the TS test loading cycle, the complex shear modulus curves of all composite modified asphalt binders show a small platform area or peak, which is due to the lower TS test temperature. When the DSR rotor began applying shear stress to the composite modified asphalt binders, the asphalt binders had not yet experienced fatigue damage, and its internal resistance to the external shear load was stronger. As the loading cycles increases, the asphalt binders internal fatigue damage is gradually occurring, and then the complex shear modulus then maintains the trend of decreasing with increasing loading cycles. The complex shear modulus and phase angle at the end of the fatigue loading cycle are marked in the graphs. The increase in the amount of NRA resulted in a significant increase in the phase angle after damage, indicating that NRA has a positive effect on improving the fatigue resistance of modified asphalt.

3.3.2. Verification of fatigue crack results of DSR-C model

By substituting the obtained results of the rheological parameters of the composite modified asphalt binders before and after fatigue damage into the DSR-C model (Eq. (9)), the calculated fatigue crack lengths of different composite modified asphalt binders can be obtained. In order to further verify the accuracy of the fatigue crack length calculated by the DSR-C model, it is necessary to obtain the real fatigue crack length of the composite modified asphalt binders at the end of the TS test with the help of image processing. The accuracy and reliability of the DSR-C model can be verified by comparing the difference between the measured and calculated values. The true fatigue crack length of the composite modified asphalt binders at the end of the TS test can be determined by the following image processing steps:

Acquisition of real fatigue crack images of asphalt binders surface after TS test. After 54,000 loading cycles of TS test, the temperature of

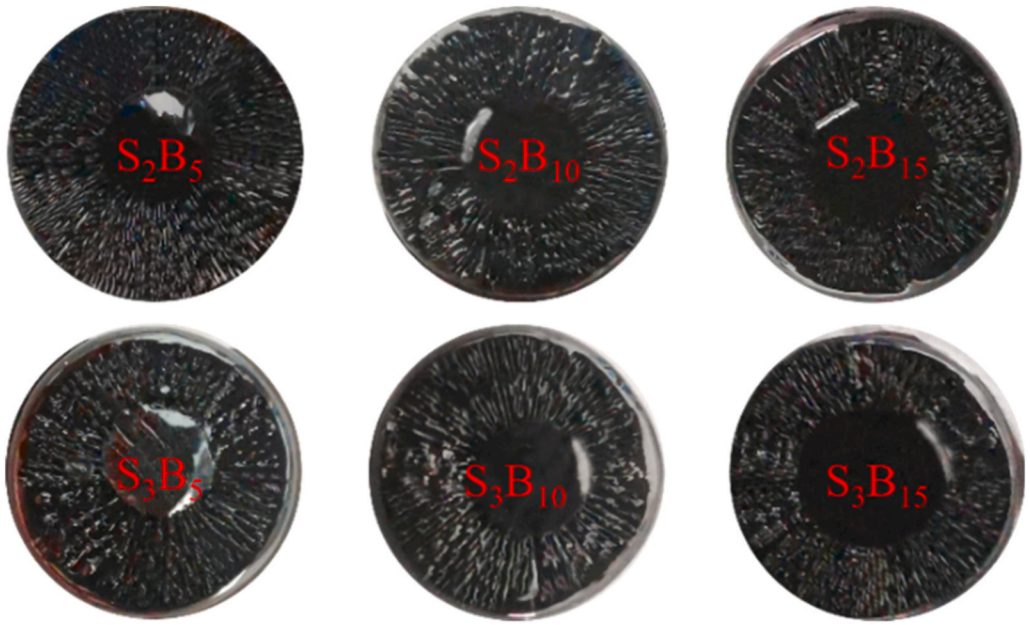

Fig. 14. Surface images of fatigue cracking of BRA/SBS at 20 °C and 10 Hz loading conditions.

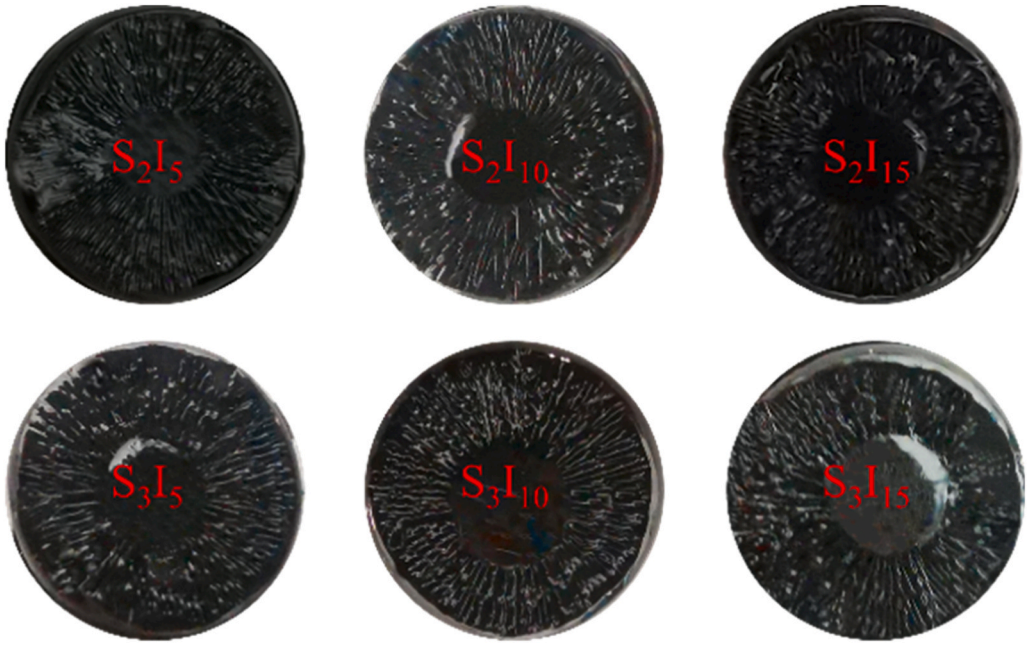

Fig. 15. Surface images of fatigue cracking of IRA/SBS at 20 °C and 10 Hz loading conditions.

DSR mainframe is set to 3 °C, and the temperature is kept at this temperature for 10 min, so that the composite modified asphalt binders will completely cool down to prevent it from melting. It can keep the geometric dimensions and internal cracks fixed. Also this step facilitate the subsequent sampling operation. At the end of the holding procedure, the 8 mm rotor is withdrawn and images of the asphalt binders surface crack morphology are taken from a fixed distance perpendicular to the asphalt binders surface direction. Fig. 13(a) shows a typical asphalt binders surface real fatigue crack morphology image obtained during this procedure. It can be seen that in the centre portion of the asphalt binders sample, a smoother circular uncracked area is presented, which is caused by the direct pull-off after the TS test.

This central region represents the uncracked portion of the asphalt binders sample during the TS test and its radius is defined as the effective radius (r_E). Around this central region, there exists an annular area of rough surfaces consisting of crests and troughs along the radial direction of the specimen as a result of shear-induced surface interactions between the bottom of the rotor and the cracked surface at the top of the specimen. It means that this annular area is caused by cracking under rotational shear loading. This type of cracking pattern is known as "roof cracking", and the surface morphology of this crack demonstrates that crack propagation in the asphalt binders samples in the DSR experiments is essentially controlled by the shear fatigue loading rather than by the "edge instability" of the specimens [31]. For the fatigue crack length is defined as labelled in Fig. 13(a), where r_0 is the asphalt binders radius and the fatigue crack length is the difference between r_0 and the effective radius r_E.

Measurement of real fatigue cracks. Firstly, the real crack

Table 6
Fatigue modelling parameters and crack length results of composite modified asphalt binders under 54,000 loading cycles.

Asphalt binder	G_0^* (kPa)	δ_0 (°)	G_N^* (kPa)	δ_N (°)	Model calculation (mm)	Measured (mm)
S_2B_5	3468.317	52.459	575.668	50.835	1.433	1.423
S_2B_{10}	3267.868	54.301	646.135	52.633	1.318	1.329
S_2B_{15}	2686.796	58.147	625.538	53.737	1.185	1.193
S_3B_5	3593.176	53.11	618.978	51.264	1.407	1.419
S_3B_{10}	3057.084	55.094	649.81	53.382	1.269	1.257
S_3B_{15}	2734.819	59.584	651.687	58.06	1.194	1.176
S_2I_5	3600.227	51.434	520.724	48.957	1.511	1.513
S_2I_{10}	3170.362	54.079	559.396	51.416	1.385	1.402
S_2I_{15}	2719.522	57.354	584.717	53.699	1.246	1.230
S_3I_5	3694.554	51.736	602.724	50.212	1.444	1.437
S_3I_{10}	3269.546	54.305	699.164	52.782	1.267	1.275
S_3I_{15}	2788.333	58.479	646.255	55.742	1.203	1.193

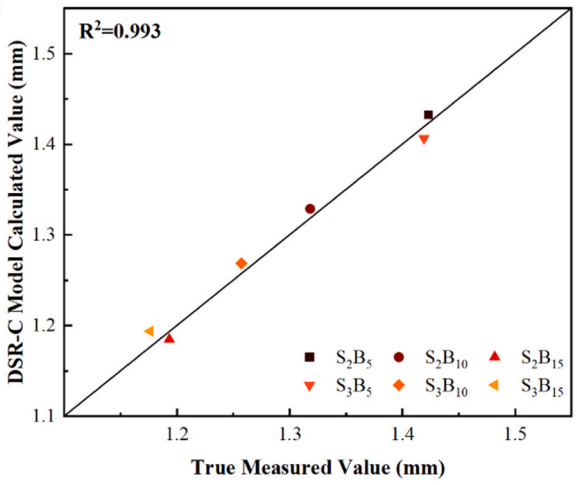

(a) BRA/SBS

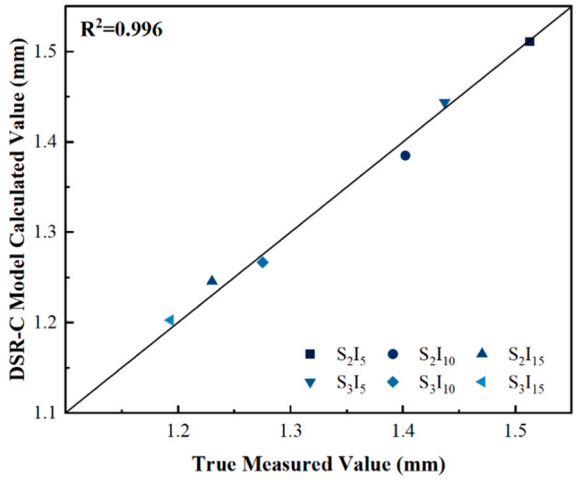

(b) IRA/SBS

Fig. 16. Correlation between calculated and measured fatigue crack values for DSR-C model at 54,000 loading cycles.

morphology image of the original asphalt binders surface is processed, in which the specific area involved is defined as shown in Fig. 14(b).

Base on the significant difference in grey values, the boundary between the undamaged area and the cracked area is marked using the Adobe Photoshop CS6 software. The pixel area of the undamaged area and the entire sample area is calculated using the pixel area statistics function in Image Pro Plus (IPP) 6.0 software, and the actual area ratio is replaced with the pixel area ratio (S_e/S_0). The final crack length (c), denoted as the measured crack length, can be obtained by Eq. (10). Figs. 14 and 15 show the fatigue-cracked surface images of BRA/SBS and IRA/SBS composite asphalt binders, respectively.

$$c = \frac{d_0(1 - \sqrt{S_e/S_0})}{2} \tag{10}$$

Where d_0 is the diameter of the sample, which is 8 mm.

According to the above process the real measured and model calculated values of fatigue damage crack length of composite modified asphalt binders based on DSR-C model can be calculated. The results are shown in Table 6. Under 54,000 cycles of loading, all the composite modified asphalt binders produce fatigue cracks of more than 1 mm.The fatigue crack lengths are reduced by the influence of the increase in the dosage of SBS and NRA. The fatigue crack true measured values can be obtained sorted as: BRA: S_3B_{15}<S_2B_{15}<S_3B_{10}<S_2B_{10}<S_3B_5<S_2B_5, IRA: S_3I_{15}<S_2I_{15}<S_3I_{10}<S_2I_{10}<S_3I_5<S_2I_5. The shorter the fatigue crack, the better the fatigue resistance.

The fatigue crack lengths of S_3I_{15} and S_3B_{15} are 1.193 mm and 1.176 mm respectively, which are only 78.85 % and 82.64 % of the fatigue crack lengths of S_2I_5 and S_2B_5. It showed that SBS and NRA effectively improved the fatigue life of composite modified asphalt binders. The correlation analysis between the calculated values of DSR-C model and the corresponding real measurements is shown in Fig. 16. The figure demonstrates that the real measurements of the fatigue crack lengths for both types of NRA and SBS composite modified asphalt

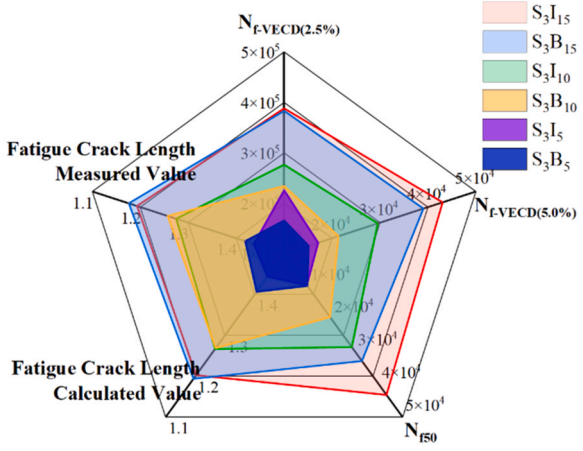

Fig. 17. Comprehensive comparison of fatigue performance index of NRA/SBS composite modified asphalt binders.

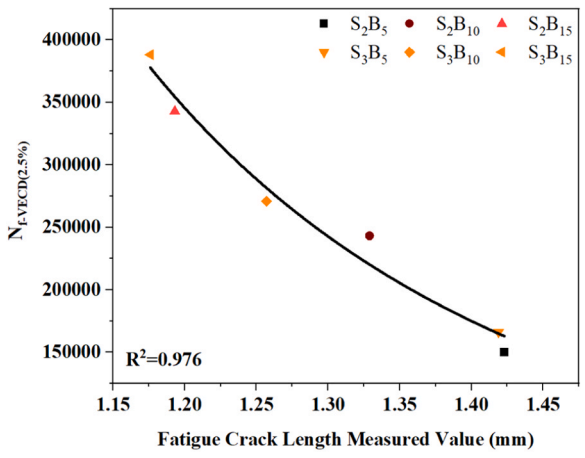

(a) BRA/SBS

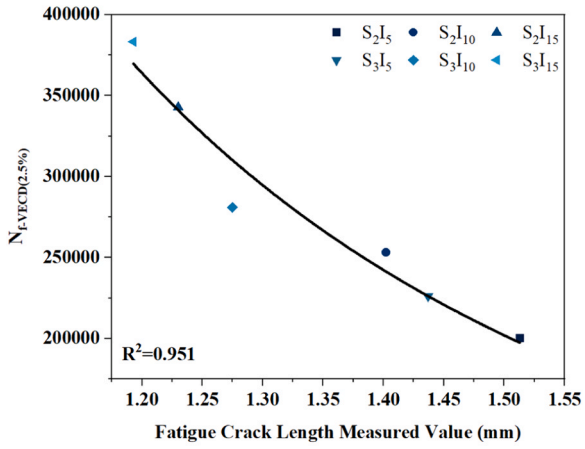

(b) IRA/SBS

Fig. 18. Measured fatigue crack value and $N_{f\text{-}VECD(2.5\ \%)}$ correlation.

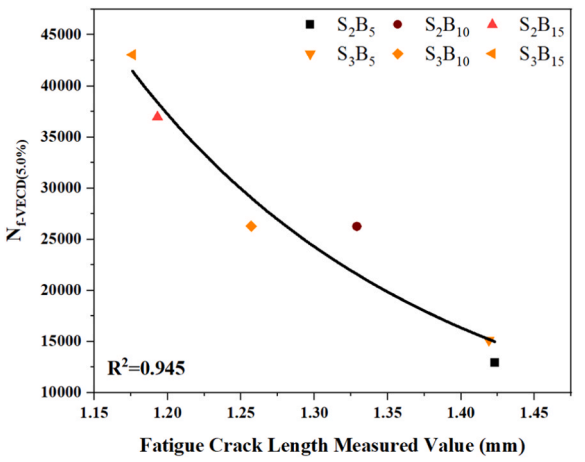

(a) BRA/SBS

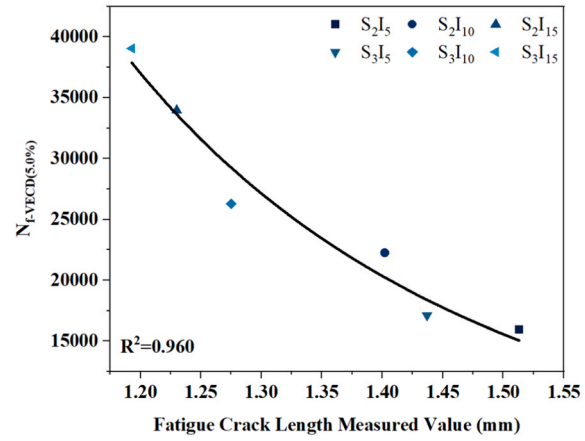

(b) IRA/SBS

Fig. 19. Measured fatigue crack value and $N_{f\text{-}VECD(5.0\ \%)}$ correlation.

binders exhibit a strong correlation with the calculated values from the DSR-C model. It suggests that the DSR-C model has a high computational accuracy and reliability.

3.4. Comprehensive comparison of different fatigue performance indexes

In order to visually compare the difference in fatigue performance between BRA/SBS composite modified asphalt binders and IRA/SBS composite modified asphalt binders, S_3B_5, S_3B_{10}, S_3B_{15}, S_3I_5, S_3I_{10}, and S_3I_{15} are selected for a comprehensive comparison. The evaluation indicators include the S-VECD fatigue life (under the strain level of 2.5 % and 5.0 %), the corresponding fatigue life based on the complex modulus decay criterion (N_{f50}), the calculated fatigue crack length of the DSR-C model and the measured fatigue crack length.

As shown in Fig. 17, the pentagonal species has five corners, including three fatigue life indexes and two fatigue crack indexes. Each corner also represents the ranking of six modified asphalt fatigue indicators. As can be seen, the fatigue performance indicators of different modified asphalts binders are essentially identical in terms of conventional fatigue life and fatigue cracking. The measured and calculated fatigue crack lengths of S_3B_5 and S_3I_5 are greater than 1.4 mm, which is much larger than the measured and calculated fatigue crack lengths of S_3B_{15} and S_3I_{15}. And it implies that S_3B_5 and S_3I_5 show a weaker resistance to fatigue crack extension during fatigue testing. The fatigue life of S_3B_{15} and S_3I_{15} under the strain level of 2.5 % and 5.0 % and the fatigue life corresponding to the complex modulus decay criterion exceeded those of S_3B_5 and S_3I_5, which indicates that the composite modified asphalt binders with the combination of 3 wt% SBS and 15 wt% NRA has a good fatigue resistance performance.

In light of the above analysis, a correlation is established between the fatigue crack indexes of the real test and the fatigue life indexes. The results of this correlation are presented in Figs. 18–20. The findings of the correlation analysis demonstrate a strong correlation between the fatigue crack indexes and the fatigue life indexes, with R^2 values exceeding 0.94. This substantiates the reliability of fatigue crack indicators in evaluating the fatigue performance of NRA/SBS composite modified asphalt binder. With the exception of the fatigue life calculated by S-VECD theory under low strain conditions, the correlation between fatigue crack index and fatigue life of IRA/SBS modified asphalt binder is higher and more significant than that of BRA/SBS modified asphalt binder. This finding indicates that the fatigue crack index is a more suitable index for evaluating IRA/SBS modified asphalt binder. It is important to note that the correlation between the fatigue cracking index and the $N_{f\text{-}VECD}$ of the BRA/SBS modified asphalt binder is weaker than the other indexes at a strain level of 5 %, with an R^2 value of 0.945. This indicates that the use of the fatigue cracking index for the evaluation of the fatigue performance of the BRA/SBS-modified asphalt binder is not precise enough at high strain conditions.

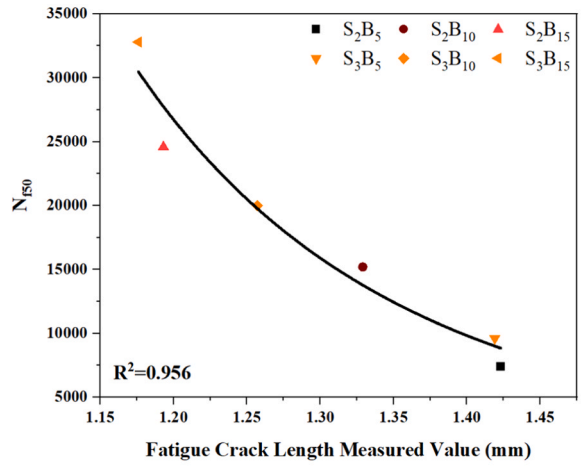

(a) BRA/SBS

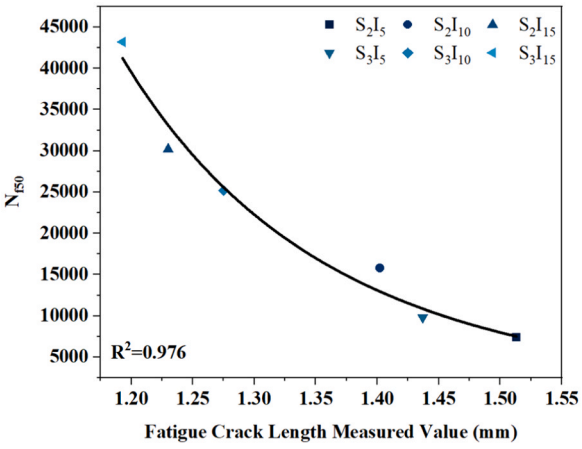

(b) IRA/SBS

Fig. 20. Measured fatigue crack value and N_{f50} correlation.

4. Conclusion

In this study, the fatigue characteristics of NRA/SBS composite modified asphalt binders based on LAS test and TS test are analysed by S-VECD model, 50 % complex modulus decay criterion, $S \times N$ peak criterion, and the DSR-C model. The fatigue damage parameters of NRA/SBS composite asphalt binders were determined both before and after fatigue testing, and the DSR-C model's crack-prediction capability was validated by comparison with actual binder crack-morphology images. The fatigue crack indexes and fatigue life indexes calculated by DSR-C model are also correlated. The main conclusions are as follows:

(1) From the results of the LAS test, it can be seen that the material integrity of the composite modified asphalt binders increases with adding BRA and IRA. For the same composite modified asphalt binders, $N_{f\text{-}VECD}$ under the strain level of 5.0 % was significantly lower than the $N_{f\text{-}VECD}$ under the strain level of 2.5 %, it is evident that high strain conditions are unfavourable to the fatigue life of composite modified asphalt binders.
(2) The TS test results show that BRA and IRA composite modified asphalt binders maintain good fatigue resistance during the test loading cycle. The increase of SBS and NRA content has a positive effect on the fatigue resistance of the composite modified asphalt binders, this may be due to the synergistic effect of NRA and SBS.
(3) The DSR-C model has good accuracy and reliability for the prediction of fatigue crack length of NRA/SBS composite modified asphalt binders, which accurately matches with the real measurements based on the real asphalt binders cracking morphology images. It can accurately reflect the fatigue crack extension process of NRA/SBS composite asphalt binders under fatigue loading conditions.
(4) The fatigue cracking index calculated based on the DSR-C model can well evaluate the fatigue performance of NRA/SBS composite modified asphalt binders, and the fatigue cracking index is better applicable to IRA/SBS composite modified asphalt binders.
(5) S_3I_{15} is better than other modified asphalt binders in both fatigue life index and fatigue cracking index, which shows that S_3I_{15} has the best fatigue damage resistance.
(6) There is some variability in the fatigue performance of NRA/SBS modified asphalt binders indicated by different fatigue indexes, but the fatigue crack indexes and conventional fatigue life indexes are more strongly correlated, and their R^2 were all greater than 0.9.

For future research, it is recommended that the fatigue performance of modified asphalt binders be evaluated from an energetic perspective to develop a more generalizable fatigue evaluation method. In addition, subsequent studies should further refine the DSR-C model and improve its accuracy to ensure its applicability to a wider range of modified asphalt binders types.

CRediT authorship contribution statement

Liang Xiong: Data curation, Writing-original draft. **Kai Liu:** Investigation, Methodology. **Huda A. Kadhim:** Writing - review & editing. **Dongyu Niu:** Supervision, Methodology, Writing - review & editing. **Yangming Gao:** Supervision, Writing - review & editing. **Xueyan Liu:** Methodology, Writing - review & editing.

Declaration of Competing Interest

The authors declare that they have no known competing financial interests or personal relationships that could have appeared to influence the work reported in this paper.

Acknowledgements

This work was supported by the Natural Science Basic Research Program of Shaanxi (2024JC-YBMS-374), the Fundamental Research Funds for the Central Universities, CHD (No. 300102314902), Shaanxi Housing and Urban-Rural Development Science and Technology Project (2023-K12), Zhengcheng R&D Center (ZCYF-2023-01-01) and the Shaanxi Provincial Key R&D Program Projects (No. 2024GX-ZDCYL-03-09).

Data availability

Data will be made available on request.

References

[1] J. Cao, Y. Zhao, W. Qiu, X. Shao, J. Cui, Coupled fatigue behavior of the steel deck plate in lightweight composite bridge decks, J. Constr. Steel Res. 223 (2024) 108999, https://doi.org/10.1016/j.jcsr.2024.108999.
[2] X. Li, J. Fu, F. Yang, H. Cao, Z. Zhang, F. Liu, Y. Li, Laboratory investigation for the bridge deck pavement performance of conventional asphalt mixtures based on fuzzy comprehensive evaluation method, Case Stud. Constr. Mater. 20 (2024) e02784, https://doi.org/10.1016/j.cscm.2023.e02784.
[3] Q. Xiang, F. Xiao, Applications of epoxy materials in pavement engineering, Constr. Build. Mater. 235 (2020) 117529, https://doi.org/10.1016/j.conbuildmat.2019.117529.
[4] H. Wang, Y. Liu, J. Li, S. Liu, J. Yang, S. Luo, W. Huang, Environmental life cycle assessment of bridge deck pavement and case studies of two bridges in China, Case Stud. Constr. Mater. 18 (2023) e02115, https://doi.org/10.1016/j.cscm.2023.e02115.

[5] L. Chen, X. Zhao, Z. Qian, X. Li, Mechanical behavior of asphalt pavement on steel-concrete composite beam bridge under temperature-load coupling, Constr. Build. Mater. 403 (2023) 133099, https://doi.org/10.1016/j.conbuildmat.2023.133099.
[6] R.G. Hicks, I.J. Dussek, C. Seim, Asphalt surfaces on steel bridge decks, Transp. Res. Rec. 1740 (1) (2000) 135–142, https://doi.org/10.3141/1740-17.
[7] C. Ai, A. Rahman, F. Wang, E. Yang, Y. Qiu, Experimental study of a new modified waterproof asphalt concrete and its performance on bridge deck, Road Mater. Pavement Des. 18 (Suppl. 3) (2017) S270–S280, https://doi.org/10.1080/14680629.2017.1329881.
[8] A. Kawakami, I. Sasaki, K. Kubo, S. Ueno, M. Hermadi, W. Pravianto, Possibility to utilize new natural rock asphalt for guss asphalt, Asph. Pavements (997) (2014) 1513–1520.
[9] W. Lu, X. Peng, S. Lv, Y. Yang, J. Wang, Z. Wang, N. Xie, High-temperature properties and aging resistance of rock asphalt ash modified asphalt based on rutting index, Constr. Build. Mater. 363 (2023) 129774, https://doi.org/10.1016/j.conbuildmat.2022.129774.
[10] S. Lv, X. Fan, H. Yao, L. You, Z. You, G. Fan, Analysis of performance and mechanism of Buton rock asphalt modified asphalt, J. Appl. Polym. Sci. 136 (1) (2019) 46903, https://doi.org/10.1002/app.46903.
[11] W.T. Huang, G.Y. Xu, Experimental study of high temperature properties and rheological behavior of Iranian rock asphalt, Adv. Mater. Res. 671 (2013) 1277–1281, https://doi.org/10.4028/www.scientific.net/AMR.671-674.1277.
[12] J. Sun, S. Luo, W. Huang, J. Hu, S. Liu, Structural optimization of steel bridge deck pavement based on mixture performance and mechanical simulation, Constr. Build. Mater. 367 (2023) 130217, https://doi.org/10.1016/j.conbuildmat.2022.130217.
[13] Y. Su, X. Hu, J. Wan, S. Wu, Y. Zhang, X. Huang, Z. Liu, Physical properties and storage stability of Buton rock asphalt modified asphalt, Materials 15 (10) (2022) 3592, https://doi.org/10.3390/ma15103592.
[14] H.U. Bahia, H. Zhai, M. Zeng, Y. Hu, P. Turner, Development of binder specification parameters based on characterization of damage behavior (with discussion), J. Assoc. Asph. Paving Technol. 70 (2001). ⟨http://worldcat.org/issn/02702932⟩.
[15] J.P. Planche, D.A. Anderson, G. Gauthier, Y.M. Le Hir, D. Martin, Evaluation of fatigue properties of bituminous binders, Mater. Struct. 37 (2004) 356–359, https://doi.org/10.1617/14127.
[16] D.A. Anderson, Y.M. Le Hir, M.O. Marasteanu, J.P. Planche, D. Martin, G. Gauthier, Evaluation of fatigue criteria for asphalt binders, Transp. Res. Rec. 1766 (1) (2001) 48–56, https://doi.org/10.3141/1766-07.
[17] L. Shan, S. Tian, H. He, N. Ren, Internal crack growth of asphalt binders during shear fatigue process, Fuel 189 (2017) 293–300, https://doi.org/10.1016/j.fuel.2016.10.094.
[18] M. Sabouri, D. Mirzaiyan, A. Moniri, Effectiveness of linear amplitude sweep (LAS) asphalt binder test in predicting asphalt mixtures fatigue performance, Constr. Build. Mater. 171 (2018) 281–290, https://doi.org/10.1016/j.conbuildmat.2018.03.146.
[19] S. Lv, S. Wang, T. Guo, C. Xia, J. Li, G. Hou, Laboratory evaluation on performance of compound-modified asphalt for rock asphalt/styrene–butadiene rubber (sbr) and rock asphalt/nano-CaCO3, Appl. Sci. 8 (6) (2018) 1009, https://doi.org/10.3390/app8061009.
[20] Y. Zhang, W. Lu, D. Han, H. Guo, X. Peng, W. Zhu, M. Xie, Laboratory investigation of modified asphalt containing Buton rock asphalt or ash from Buton rock asphalt, Case Stud. Constr. Mater. 18 (2023) e02124, https://doi.org/10.1016/j.cscm.2023.e02124.
[21] JTG E20-2011, Standard Test Methods of Bitumen and Bituminous Mixtures for Highway Engineering.
[22] JT/T 860.5-2014, Modifier for Asphalt Mixture-Part 5: Natural Asphalt.
[23] Y. Wen, N. Guo, L. Wang, B. Jiao, W. Li, Rheological properties and microscopic mechanism of rock asphalt composite modified asphalts, Constr. Build. Mater. 281 (2) (2021) 122543, https://doi.org/10.1016/j.conbuildmat.2021.122543.
[24] F. Xiao, S.N. Amirkhanian, M. Karakouzian, M. Khalili, Rheology evaluations of wma binders using ultraviolet and pav aging procedures, Constr. Build. Mater. 79 (March 15) (2015) 56–64, https://doi.org/10.1016/j.conbuildmat.2015.01.046.
[25] C. Hintz, H. Bahia, Simplification of linear amplitude sweep test and specification parameter, Transp. Res. Rec. 2370 (1) (2013) 10–16, https://doi.org/10.3141/2370-02.
[26] S.W. Park, Y.R. Kim, R.A. Schapery, A viscoelastic continuum damage model and its application to uniaxial behavior of asphalt concrete, Mech. Mater. 24 (4) (1996) 241–255, https://doi.org/10.1016/s0167-6636(96)00042-7.
[27] Y. Zhang, Y. Gao, Predicting crack growth in viscoelastic bitumen under a rotational shear fatigue load, Road Mater. Pavement Des. (2019), https://doi.org/10.1080/14680629.2019.1635516.
[28] F. Ma, C. Zhang, Road performance of asphalt binder modified with natural rock asphalt, Adv. Mater. Res. 634-638 (2013) 2729–2732, https://doi.org/10.4028/www.scientific.net/AMR.634-638.2729.
[29] C. Wang, C. Castorena, J. Zhang, Y. Richard Kim, Unified failure criterion for asphalt binder under cyclic fatigue loading, Road Mater. Pavement Des. 16 (Suppl. 2) (2015) S125–S148, https://doi.org/10.1080/14680629.2015.1077010.
[30] C. Wang, H. Zhang, C. Castorena, J. Zhang, Y.R. Kim, Identifying fatigue failure in asphalt binder time sweep tests, Constr. Build. Mater. 121 (2016) 535–546, https://doi.org/10.1016/j.conbuildmat.2016.06.020.
[31] Y. Gao, L. Li, Y. Zhang, Modelling crack initiation in bituminous binders under a rotational shear fatigue load, Int. J. Fatigue 139 (2020) 105738, https://doi.org/10.1016/j.ijfatigue.2020.105738.